Experimentation with curvature sensing

Erez Ribak* and Shirly Vinikman
Department of Physics
Technion - Israel Institute of Technology
Technion City, Haifa 32000, Israel
*eribak@physics.technion.ac.il

ABSTRACT

Curvature sensing is a non-interferometric wave front sensing method. In order to understand its applicability we tested it in a controlled laboratory environment. We tried various optical configurations and different data processing methods, such as Projection on Convex Sets and Finite Elements. Repeatability between different configurations and analysis methods is to within eight percent.

1. Beam propagation

We start with a wave propagating in the $+z$ direction:

$$u(x,y,z,t) = \exp(-i2\pi t / \lambda)u_z(\mathbf{r}), \quad \mathbf{r} = (x,y).$$

We express u_z in terms of real intensity (or irradiance) and phase $u_z(\mathbf{r}) = \left[I_z(\mathbf{r}) \right]^{1/2} \exp\left[i\,\varphi(\mathbf{r}) \right]$. The paraxial equation is

$$\Pi = \left(i\frac{\partial}{\partial z} + \frac{\nabla^2}{2k} + k \right)u_z(\mathbf{r}) = 0,$$

where $\nabla^2 = \partial/\partial x^2 + \partial/\partial y^2$; $k = 2\pi/\lambda$. If $\Pi = 0$ then also $\Pi u_z^* - u_z \Pi^* = 0$, and we get the Transport of Intensity Equation (TIE), also known as the Irradiance Transport Equation [7, 6]:

$$k\frac{\partial}{\partial z}I(\mathbf{r},z) = -\nabla \cdot \left[I(\mathbf{r},z)\nabla\,\varphi(\mathbf{r},z) \right].$$

This equation ties intensity and phase values along the optical propagation path.

2. Curvature sensing

If $I(x,y,z = 0) = I_0 = \text{const}$, the ITE reduces to

$$-\frac{k}{I_0}\frac{\partial I}{\partial z} = \nabla^2\,\varphi + \delta(e)\frac{\partial\varphi}{\partial n}; \quad e = edge,$$

combined with Neumann boundary conditions $\partial\varphi / \partial n$ measured through the *intensity* around $\delta(e)$. We approximate the longitudinal derivative as

$$\frac{1}{I_0}\frac{d}{dz} \approx \frac{I(z-\Delta z)-I(z+\Delta z)}{I_0 \cdot 2\Delta z} \approx \frac{1}{\Delta z}\frac{I(z-\Delta z)-I(z+\Delta z)}{I(z-\Delta z)+I(z+\Delta z)}.$$

We constructed an optical system that allows us to re-image different planes on the camera (Figure 1). By moving the lens in front of the camera, we can choose the two planes to overlap (before and after reflection from the sample), or at any two other locations.
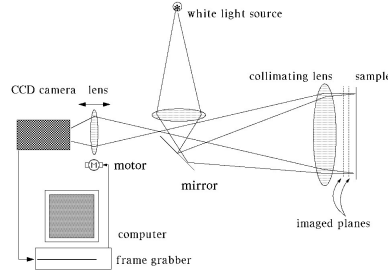

Figure 1: Optical system for measuring reflected wave fronts (full image).

In order to solve the TIE we use the Fourier relationship $FT\{\wp\} = \omega^{-2}FT\{\nabla^2\wp\}$, where ω is the spatial frequency [5, 2]. However, to apply that we also need to plug in the boundary conditions. This is done by defining a slightly larger domain. We rewrite the TIE with an additional term, whose value is equal to zero:

$$-\frac{k}{I_0}\frac{d}{dz} = \nabla^2\wp + \delta(e)\frac{\partial\wp}{\partial n} - \delta(e+\Delta)\frac{\partial\wp}{\partial n}.$$

The last two terms can now be absorbed into the laplacian:

$$-\frac{k}{I_0}\frac{d}{dz} = \nabla^2\wp,$$

subject to the boundary conditions $\partial\wp/\partial n = 0$ around $\delta(e+\Delta)$. The equation is solved by the method of Projection on Convex Sets, by repeatedly entering the measured intensity signals inside the boundary, finding the phase, applying the boundary conditions, and so on [2, 5]. This is shown in Figure 2.

In our experimental setup, we are interested in local details. The wave front might be tilted, have global curvature, or other aberrations on a large scale. This is of low importance if one is looking for small-scale details. To get rid of global aberrations, we fit by least-squares the wave front to Zernike polynomials, and remove them [4]. In Figure 3, we show a cut through a deformable mirror under different voltages. Global tip and tilt have been removed, and the most obvious effect is the curvature change. While testing deformable mirrors, we were able to achieve repeatability of 5%, and local accuracy of few Ångstroms [1]. Our ability to improve this accuracy requires better optics, fine alignment of the measurement planes, and a better digitizing camera (we currently use standard, inexpensive optical and electronic equipment).
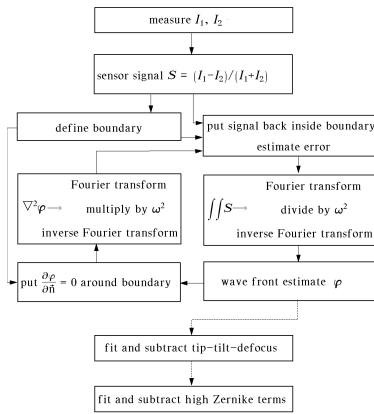
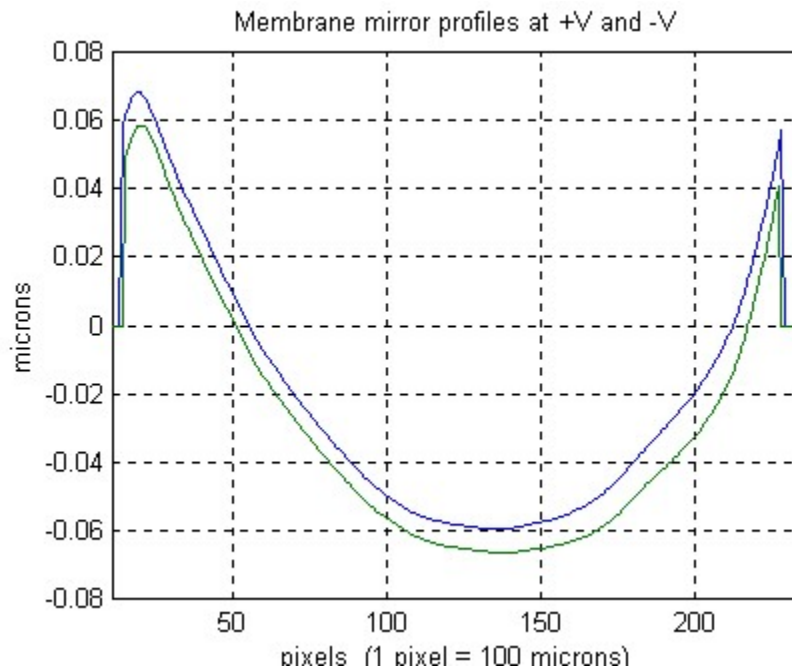**Figure 2: Processing of data: iterative enforcement of signal and of boundary conditions ([full image](#)).**

Figure 3: Cuts through a flexible mirror under electric field.

-

---

3. Phase sensing in two planes

We start again with the assumption that the intensity is constant before hitting the first distorting surface. The TIE can now be approximated (for small distortions) by

$$\frac{dI(\mathbf{r},z)}{I(\mathbf{r},z)} = d\ln I(\mathbf{r},z) \approx -\frac{1}{k}dz\nabla^2\phi(\mathbf{r},z).$$

Upon integration, we only consider distortions in two planes, say z_1 and z_2, and neglect them elsewhere. If I_0 is the initial intensity, then

$$-k\ln\frac{I(\mathbf{r})}{I_0} \approx z_1\nabla^2\phi_1(\mathbf{r},z_1) + z_2\nabla^2\phi_2(\mathbf{r},z_2).$$

If either one of the planes is close to the observation plane, we see that most of the intensity changes will be due to the other plane. This is exactly the case of astronomical scintillation, created by distant turbulent layers [3].

By judicious choice of the detection plane, one can be sensitive to either distorting plane. Imaging one of the planes on the detector, it has no effect on the intensity fluctuations. Only the distortions in the second plane are measured. The opposite is also true: focusing on the second plane, intensity scintillation will be a result of phase variations in the first.

The detector signal, to be fed into the phase recovery algorithm, is

$I(z-\Delta z) - I(z+\Delta z)/I(z-\Delta z) + I(z+\Delta z)$. The denominator is actually the intensity (with scintillation imposed on it), which is being normalized away. However, it would be more beneficial to use this intensity to estimate the phase fluctuations in the other plane [3]. Thus, four images are to be taken: two, just before and after the first plane, and two, just before and after the second plane. It might be possible to reduce the number of measurements in special cases.

References

1. Barty, A, K A Nugent, D Paganin, and A Roberts, �Quantitative optical phase microscopy�, *Optics Letters* **23**, 817-9 (1998).
2. Restaino, S R, �Wave-front sensing and image deconvolution of solar data�, *Applied Optics* **35**, 7442-9 (1992).
3. Ribak, E N, E Gershnik, and M Cheselka, �Atmospheric Scintillations as a Remote Wave-front Sensor�, *Optics Letters* **21**, 435-7 (1996).
4. Roddier, C, and F Roddier, �Wave Front Reconstruction from Defocused Images and the Testing of Ground-Based Optical Telescope�, *J Opt Soc Am A* **10**, 2277-87 (1993).
5. Roddier, F, and C Roddier, �Wave Front Reconstruction Using Iterative Fourier Transforms�, *Applied Optics* **30**, 1325-27 (1991).
6. Streibl, N, �Phase Imaging by the Transport Equation of Intensity�, *Optics Communications* **49**, 6-10 (1984).
7. Teague, M R, �Deterministic Phase Retrieval: A Green's Function Solution�, *J Opt Soc Am* **73**, 1434-41 (1983).